applied system innovation

MDPI

Article

Machine Learning Based Predictive Modeling of Electrical Discharge Machining of Cryo-Treated NiTi, NiCu and BeCu Alloys

Vijaykumar S. Jatti [1,*], Rahul B. Dhabale [1], Akshansh Mishra [2], Nitin K. Khedkar [1,*], Vinaykumar S. Jatti [1] and Ashwini V. Jatti [1]

[1] Symbiosis Institute of Technology, Symbiosis International (Deemed) University, Pune 412115, India
[2] School of Industrial and Information Engineering, Politecnico Di Milano, 20133 Milan, Italy
* Correspondence: vijaykumar.jatti@sitpune.edu.in (V.S.J.); dydirectoradministration@sitpune.edu.in (N.K.K.)

Abstract: The advancement in technology has attracted researchers to electric discharge machining (EDM) for providing a practical solution for overcoming the limitations of conventional machining. The current study focused on predicting the Material Removal Rate (MRR) using machine learning (ML) approaches. The process parameters considered are namely, workpiece electrical conductivity, gap current, gap voltage, pulse on time and pulse off time. Cryo-treated workpiece viz, Nickel-Titanium (NiTi) alloys, Nickel Copper (NiCu) alloys, and Beryllium copper (BCu) alloys and cryo-treated pure copper as tool electrode was considered. In the present research work, four supervised machine learning regression and three supervised machine learning classification-based algorithms are used for predicting the MRR. Machine learning result showed that gap current, gap voltage and pulse on time are most significant parameters that effected MRR. It is observed from the results that the Gradient boosting regression-based algorithm resulted in the highest coefficient of determination value for predicting MRR while Random Forest classification based resulted in the highest F1-Score for obtaining MRR.

Keywords: electrical discharge machine; nickel-titanium alloys; nickel copper alloys; beryllium copper alloys; machine learning

Citation: Jatti, V.S.; Dhabale, R.B.; Mishra, A.; Khedkar, N.K.; Jatti, V.S.; Jatti, A.V. Machine Learning Based Predictive Modeling of Electrical Discharge Machining of Cryo-Treated NiTi, NiCu and BeCu Alloys. *Appl. Syst. Innov.* **2022**, *5*, 107. https://doi.org/10.3390/asi5060107

Academic Editors: Giuseppe Mangioni and Subhas Mukhopadhyay

Received: 11 September 2022
Accepted: 18 October 2022
Published: 26 October 2022

1. Introduction

Newly developed materials namely, Nickel Titanium (NiTi) alloy, Nickel Copper (NiCu) alloy, Beryllium Copper (BeCu) alloy have superior material properties including high hardness, therefore these materials are difficult to machine by conventional machining processes. Electrical discharge machining (EDM) is one of the practical solution methods for machining hard materials [1–5]. The complexity of EDM process led the researchers to take a lot of effort for finding the optimum process parameters [6–12]. The key point of research has been to develop an efficient system that leads to a higher material removal rate. On other occasions regarding using ML approaches, several techniques were used to investigate the process output, such as MRR and predictive model of EDM operations. Shukla and Priyadarshini [13] successfully used a gradient descent method as ML algorithm simultaneously optimise surface roughness and kerf width. It was seen that pulse on and off times and peak current significantly affect the roughness and width of the kerf. Ghosh et al. [14] used four ML algorithms to comprehend and model the manufacturing process of (EDM) equipment products to increase productivity. The Random Forest, Support Vector Regression, Elastic Net, and Bagging have been adopted in this study. The results justified using ML methods to deal with the research problem. Ulas et al. [15] modelled wire EDM of aluminium alloy using several ML algorithms. The study indicated that the weighted extreme learning machine (WELM) model achieved the best results with an R^2 of more than 97%. Ali et al. [16] studied the effect of EDM process parameters on MRR during

machining of BeCu. They found peak current affected the most followed by pulse on time, pulse off time and machine voltage had less effect on MRR. Selvakumar et al. [17] used RSM experimental plan to investigate the effect of peak current, workpiece thickness, pulse on time, and pulse frequency on MRR and SR during EDM of NiCu. Author's found all process parameters effect the MRR and SR. Kumar et al. [18] studied the effect of servo voltage, pulse on time, pulse on time and discharge current on MRR and SR during machining of NiCu. They have used RSM experimental plan and desirability concept for optimization. Kumar and Babu [19] employed minimum quantity dielectric based EDM setup to machine NiCu and investigated the effect of wire feed, water flow rate, pulse on time, pulse off time, air inlet pressure on MRR and SR. Daneshmand et al. [20] studied the productivity and surface integrity namely rate of tool wear, surface roughness, material removal rate and relative electrode wear during EDM of NiTi by considering discharge current, discharge voltage, pulse on time and pulse off time. MRR is effected by discharge current and pulse on time. Tool wear rate increases with increase in pulse on time upto threshold and then decreases. Surface roughness increases with increase in discharge current. MRR and SR decreases with increase in pulse off time. Gangele et al. [21] investigated the effect of EDM process parameters on SR while machining of NiTi. They found that pulse off time has more positive effect in decreasing SR. Daneshmand et al. [22] during EDM of NiTi-60 SMA studied the effect of tool rotation, Al_2O_3, voltage, current, pulse on time and pulse off time on MRR and SR. MRR decreases with voltage & pulse off time and MRR increases with current and pulse on time. TWR and SR are effect by all process parameters. Pogrebnjak et al. [23] discussed the review of ion implantation of superplastic NiTi shape memory alloys to enhance the surface properties. There are very few articles or research activities which focused on the implementation of Machine Learning algorithms in EDM process for predicting the Material Removal Rate. The present study combined experimental data obtained from the assessment of material removal rate during EDM of NiTi alloy, NiCu alloy & BeCu alloy and exposed them to supervised machine learning classification and regression-based methods.

2. Understanding Supervised Machine Learning Algorithms

A training set is used in supervised learning to instruct models to produce the desired results. This training dataset has both the right inputs and outputs, enabling the model to develop over time. The loss function serves as a gauge for the algorithm's correctness, and iterations are made until the error is sufficiently reduced. When using data mining, supervised learning may be divided into two categories of issues: classification and regression. In order to accurately classify test data into different categories, classification uses an algorithm. It identifies particular entities in the dataset and makes an effort to determine how those things should be defined or labeled. Linear classifiers, support vector machines (SVM), decision trees, k-nearest neighbor, and random forests are examples of common classification algorithms. To comprehend the relationship between independent and dependent variables, regression is used. It is frequently used to produce estimates, including those for a company's sales revenue. Popular regression algorithms include linear regression, logistical regression, and polynomial regression.

The bagging method serves as the foundation for Random Forest, which employs ensemble learning. The outcome of all the trees is combined once as many trees as possible have been created on the subset of data. In doing so, it lessens the issue of overfitting in decision trees, as well as lowering variance and raising accuracy. In contrast to decision trees, which only build one tree, Random Forest creates many trees and integrates their results. It builds 100 trees in the Python Sklearn module by default. This algorithm needs a lot more resources and computing power to accomplish this. The decision tree, on the other hand, is straightforward and doesn't need as much computing power. Compared to decision trees, Random Forest requires much more time to train since it generates many trees (instead of just one tree) and bases decisions on the majority of votes.

Although decision trees do not simultaneously take into consideration numerous weighted combinations, they have the benefit of not requiring any feature modification when working with non-linear data. One of the quickest ways to determine the most important factors and relationships connecting a group of variables is to use a decision tree. We can add new variables or features to the result variable more effectively using decision trees. Because there is no outside influence or impact from missing data in a tree node when using a decision tree, less data is needed. The time complexity for performing this operation is extremely high and keeps rising as the number of records rises. Training a decision tree with numerical variables can take a long time. Overfitting of data is typically required for decision trees. The output variance in the overfitting problem is extremely high, which causes numerous errors in the final estimation and can result in output that is extremely inaccurate. Obtaining zero bias will result in large variance (overfitting). Small alterations in the data in a decision tree may result in the generation of a complicated new tree. In the decision tree, this is referred to as variance, and it can be reduced using techniques like bagging and boosting.

The gradient boosting trees and random forests differ from one another primarily in two ways. We train the former in a systematic manner, correcting the mistakes of the prior trees with each new tree. In contrast, we independently build each tree in a random forest. As a result, we are unable to train the gradient-boosting trees in parallel whereas we can train a forest.

The simplest definition of artificial neural networks (ANN) is a model of the human brain made up of neurons. The human brain contains roughly 100 billion neurons. Between 1000 to 100,000 connections exist between each neuron. Information is distributed stored in the human brain, allowing us to simultaneously access multiple pieces of information from memory as needed. The statement that a human brain is composed of thousands of extremely potent parallel processors is accurate. Following ANN training, the data may still produce output with missing information. The degree to which the performance is lost here depends on how critical the missing data is. Determining the examples and teaching the network in accordance with the desired output by providing it with these examples is important for ANN to be able to learn. The network's performance is directly correlated with the instances chosen, and if the network is unable to see an event from all angles, it may offer inaccurate results. According to their structure, artificial neural networks demand processors with parallel processing power. The equipment's actualization is therefore dependent on this. For choosing the structure of artificial neural networks, there is no set rule. Experience and trial-and-error are required to arrive at an appropriate network structure. ANNs are capable of processing numerical data. Prior to using ANN, problems must be converted into numerical numbers. The network's performance will be directly impacted by the display mechanism chosen in this case. This is based on the user's skill.

3. Materials and Methods

Experiments were carried out on a die sink type electrical discharge machine, of Electronica Machine Tool Limited (Pune, India), model C400x250. Commercial grade EDM oil was used as dielectric fluid with side-wise flushing and 0.5 kg/cm^2 flushing pressure. NiTi alloy and NiCu alloy of Ø20 mm and length of 20 mm were used whereas BeCu of size $20 \times 20 \times 30$ mm^3 were used. The tool material selected for experimentation was electrolytic copper due to its high electrical conductivity of 6 mm diameter and 90 mm length. Prior to conducting the experiments, both the workpiece and tool were cryogenically treated. Experimental layout was design as per Taguchi L_{18} orthogonal array for conduction of experiments. Table 1 depicts the thermal and electrical conductivity of workpiece and tool electrode before and after cryogenic treatment. Table 2 shows the Taguchi L_{18} orthogonal array and obtained experimental results.

Table 1. Thermal and electrical conductivity of workpiece and tool.

Properties	NiTi Alloy		NiCu Alloy		BeCu Alloy		Copper Electrode	
	Untreated	Treated	Untreated	Treated	Untreated	Treated	Untreated	Treated
Thermal conductivity (k), W/mk	10	12.9	21.8	22.2	130	135.9	391.1	
Electrical conductivity (σ), S/mm	3.268	4.219	5.515	5.625	5.645	5.902	10	26.316

Table 2. Experimental Layout with trial conditions and observed value.

Workpiece Name and Treatment	Workpiece Electrical Conductivity (S/m)	Gap Current (A)	Gap Voltage (V)	Pulse On Time (µs)	Pulse Off Time (µs)	Material Removal Rate (mm^3/min)
NiTi Untreated	3268	8	40	13	5	2.09
NiTi Untreated	3268	12	55	26	7	4.56
NiTi Untreated	3268	16	70	38	9	7.11
NiTi Treated	4219	8	40	26	7	3.96
NiTi Treated	4219	12	55	38	9	6.5
NiTi Treated	4219	16	70	13	5	4.16
NiCu Untreated	5515	8	55	13	9	2.76
NiCu Untreated	5515	12	70	26	5	3.33
NiCu Untreated	5515	16	40	38	7	9
NiCu Treated	5625	8	70	38	7	3.1
NiCu Treated	5625	12	40	13	9	5.98
NiCu Treated	5625	16	55	26	5	6.26
BeCu Untreated	5645	8	55	38	5	3.41
BeCu Untreated	5645	12	70	13	7	3.08
BeCu Untreated	5645	16	40	26	9	9.08
BeCu Treated	5902	8	70	26	9	2.8
BeCu Treated	5902	12	40	38	5	6.7
BeCu Treated	5902	16	55	13	7	6.03

Material removal rate (MRR) is computed using Equation (1). Weighing is done before and after machining of the workpiece. This is done by utilizing a digital weighing balance of model- GR-300 with an accuracy of 0.0001 g.

$$MRR = \frac{\Delta W}{\rho_w \times t_m} \quad (1)$$

where ΔW is change in weight of work piece in grams, ρ_w is work piece density, gm/cm^3, t_m is machining time in mins.

For this study, sensitivity for anti-arc and servo motors was set at 50% and 25%, respectively. Depending on the favourable machining conditions, the workpiece and the tool were used as the negative and positive electrodes, respectively. Therefore, reverse polarity is considered in all experiments. The formulation of operational ranges for process parameters is based on literature review, favourable machining conditions, and sparks existence. In the study, instead of keeping the machining time as constant, each experiment was performed till 5 mm depth was achieved on the work piece.

In this study the experimental layout was considered as per Taguchi method. There are five input parameters namely workpiece electrical conductivity with six level and other parameters at three levels viz, gap current, gap voltage, pulse on time and pulse off time. The nearest orthogonal array that will satisfies the criterion of selecting the orthogonal array is mixed L_{18} ($6^1 \times 3^4$) orthogonal array having seventeen degrees of freedom. The experimental results obtained as per Taguchi Experimental layout was used in Machine learning as dataset for prediction of material removal rate based on regressor and classification based approaches.

The present study utilized four supervised machine learning regression-based algorithms i.e., Random Forest, Decision Tree, Gradient Boosting and Artificial Neural Network developed by Python programming for predicting the Material Removal Rate. In the present study, three supervised machine learning classification-based algorithms i.e., Decision Tree algorithm, Random Forest Algorithm, and AdaBoost algorithms are employed for classification of Material Removal Rate. If Material Removal Rate is below 5 mm^3/min then it is labeled as '0' and vice versa. Figure 1a represents the flowchart for implementing the Supervised Machine Learning algorithms on the dataset. The dataset was split into two parts i.e., the training set and testing set out of which 80% of dataset points were used for training purposes and 20% of dataset points were used for testing purposes. In the ANN model, the number of epochs employed was 2000. Figure 1b shows the feature importance graph. It is observed from the graph that one of the experimental input parameters i.e., Pulse off Time and Workpiece Electrical Conductivity were not contributing to the output parameter. So, in the present study, the main contributing input parameters are Gap Current, Gap Voltage, and Pulse On time, while Material Removal Rate is the output parameter. Figure 1c shows the heatmap plot of the experimental dataset. A heatmap uses a warm-to-cool color combination to graphically represent visitor behavior data as hot and cold regions. Light color is the location with the maximum visitor contact, and warm colors point to those areas, dark colors denote those areas with the least visitor interaction.

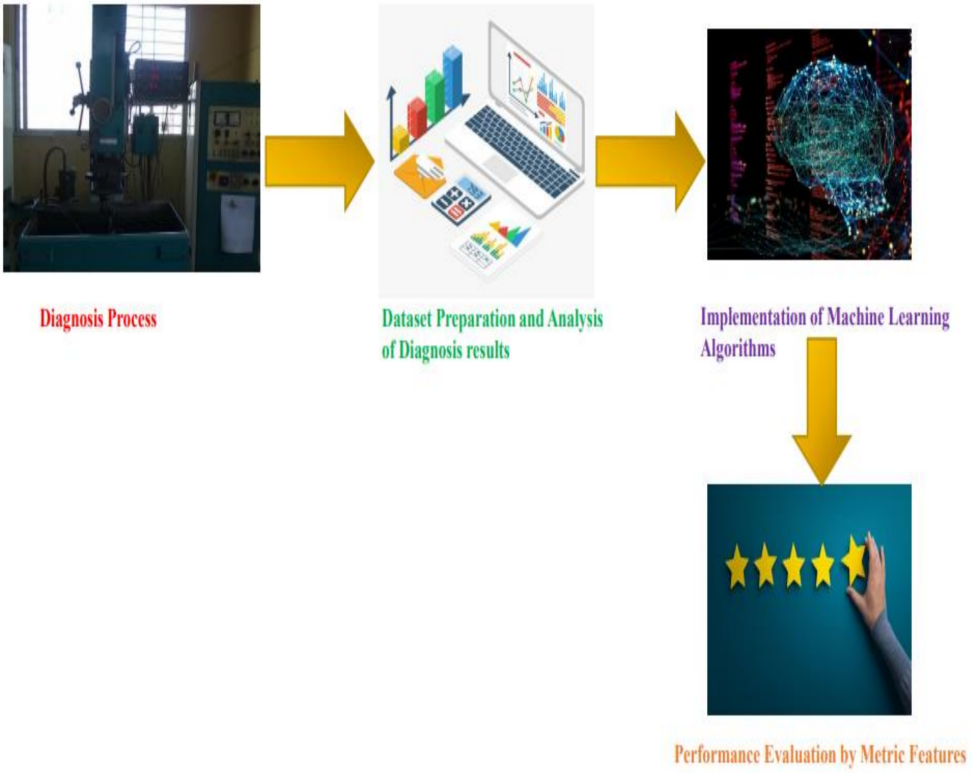

(**a**)

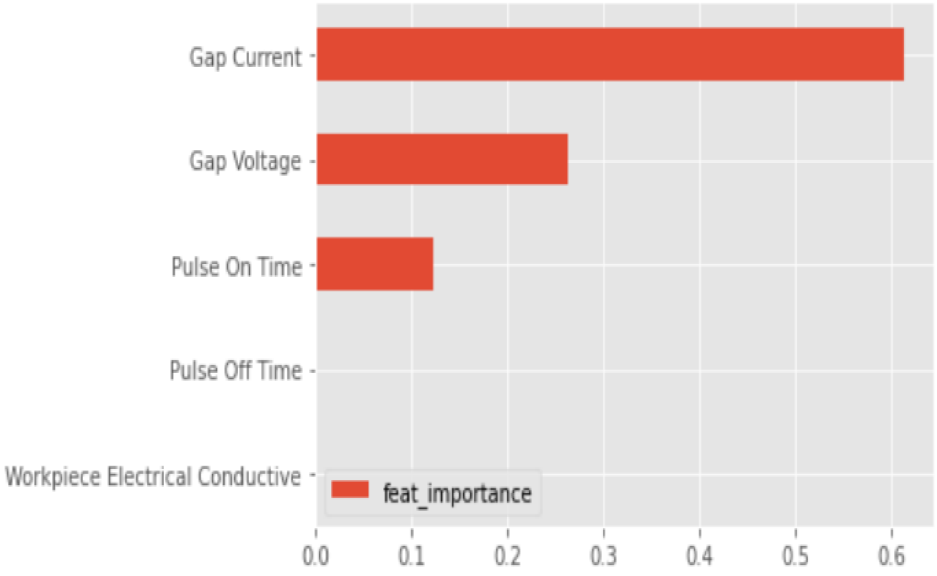

(**b**)

Figure 1. *Cont.*

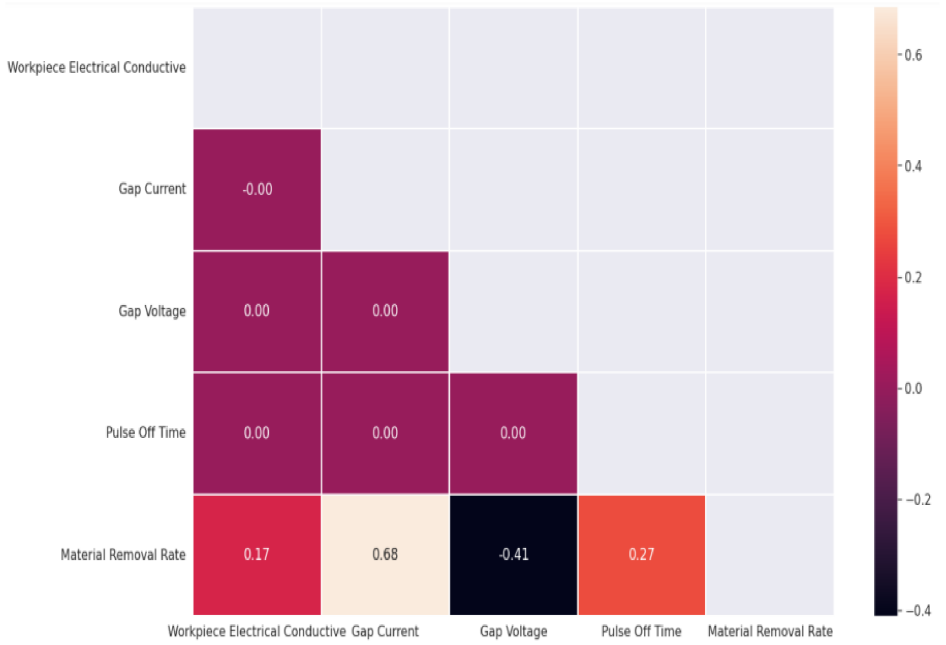

(**c**)

Figure 1. (**a**) Implementation of Machine Learning algorithms on the dataset; (**b**) Feature Importance Plot; (**c**) Heatmap representation.

4. Results

Python programming language was implemented for developing these regressions and classification-based algorithms. Metric features such as Mean Square Error (MSE), Mean Absolute Error (MAE), and coefficient of determination (R^2) are used for measuring the performance of the employed supervised machine learning algorithms. Figure 2a shows the plot of loss function of Artificial Neural Network model with increasing number of epochs. While evaluating the performance of classification-based algorithms, the F1-Score and area under curve (AUC) scores of each algorithm are evaluated. Equation (2) is used for the calculation of the F1-Score value.

$$F1\text{-}Score = 2 \times \frac{precision \times recall}{precision + recall} \quad (2)$$

Tables 3 and 4 shows the obtained results for Supervised Machine learning based regression and classification algorithms.

Table 3. Metrics features of Regression Based Algorithms.

Algorithms	Mean Square Error	Mean Absolute Error	R^2
Random Forest	0.745	0.764	0.856
Decision Tree	0.965	0.792	0.814
Gradient Boosting	0.360	0.529	0.930
Artificial Neural Network	0.255	0.098	0.749

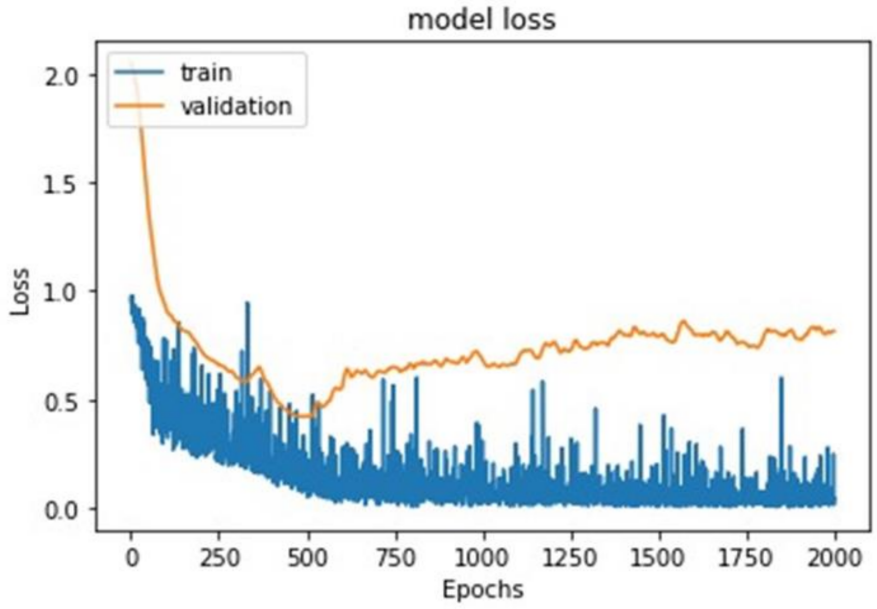

(**a**)

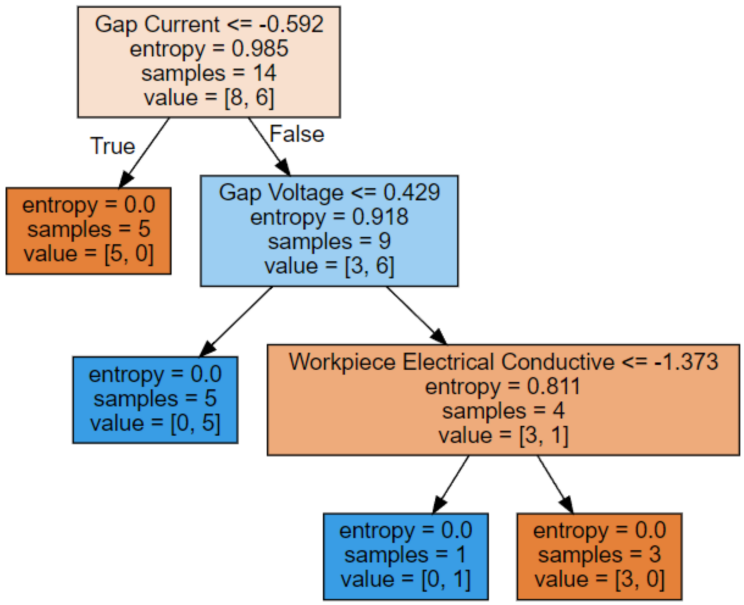

(**b**)

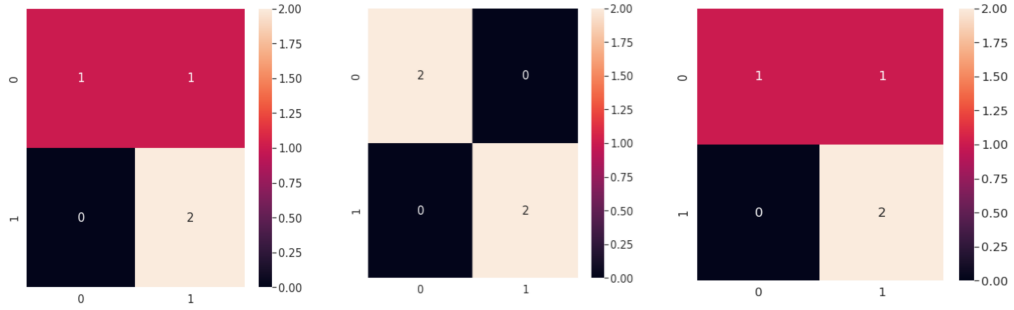

(i) (ii) (iii)

(**c**)

Figure 2. *Cont.*

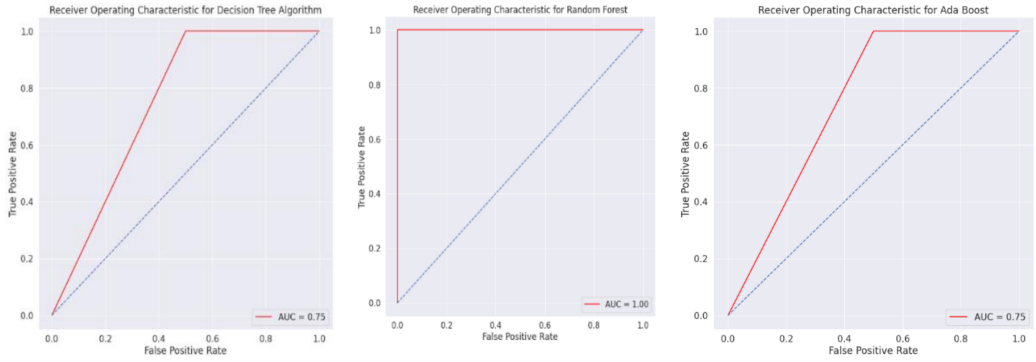

(i) (ii) (iii)

(**d**)

Figure 2. (**a**) Variation of Loss function with respect to number of epochs; (**b**) Decision Tree Classification Plot; (**c**) Confusion Matrix plot (i) Decision Tree (ii) Random Forest (iii) Ada-Boost; (**d**) ACU Curve (i) Decision Tree (ii) Random Forest (iii) Ada-Boost.

Table 4. Metrics features of Classification Based Algorithms.

Algorithms	Precision Value of '0'	Precision Value of '1'	Recall Value of '0'	Recall Value of '1'	Overall F1-Score
Decision Tree	1.00	0.67	0.50	1.00	0.75
Random Forest	1.00	1.00	1.00	1.00	1.00
AdaBoost	1.00	0.67	0.50	1.00	0.75

In the Decision Tree classification-based algorithm, entropy is used as a criterion which is calculated by Equation (3). Entropy is a unit of measurement for information that depicts the unpredictability of the target's features. The feature with the lowest entropy selects the optimal split, just like the Gini Index does. A node is pure when the entropy has its lowest value, which is zero, and it reaches its largest value when the probabilities of the two classes are equal. Figure 2b represents the obtained Decision Tree plot of the present work.

$$Entropy = -\sum_j p_j \cdot log_2 \cdot p_j \quad (3)$$

where p_j stands for class j probability.

5. Discussion

From Figure 1b it is observed from the graph that one of the experimental input parameters i.e., Pulse off Time and Workpiece Electrical Conductivity were not contributing to the output parameter. So, in the present study, the main contributing input parameters are Gap Current, Gap Voltage, and Pulse On time on Material Removal Rate.

With an increase in gap current, MRR increases regardless of whether or not the work piece is cryogenically treated. Increasing the gap current will increase the effective energy available in the machining area. A high gap current is reported to give a high current density. Furthermore, the expansion of the dielectric medium causes an increase in the impulsive force, allowing the working materials to melt and evaporate. Positive ions attack the workpiece surface more readily when the gap current increases. Consequently, the surface temperature of the workpiece rises, melting or evaporating the material. As a result, the crater size increases leading to a higher MRR. With an increase in gap current, the MRR also increases, and cryogenic treatment can further enhance the MRR value.

When the gap voltage is lower, the inter electrode spark gap will be smaller. If debris accumulates at the interface between the tool and the work piece, it will cause damage. This leads to arcing, which results in the electrodes becoming corroded. Gap voltage affects

spark energy, which is well known. Low gap voltage reduces spark energy and results in a lower material removal rate.

The MRR is typically directly related to the discharge energy, which is determined by pulse duration. Increasing pulse duration will lead to greater discharge energy. A greater number of positive ions from the plasma channel strike the work surface. As a result of the bombardment of ions, the surface temperature of the work piece increases. Hence, the rise in temperature melts work material and increases MRR.

From Table 2 it is observed that the Gradient boosting algorithms yields a lower value of MSE and MAE value with a highest value of the coefficient of determination (R^2) i.e., 0.93. In light of this, it can be observed that Gradient Boosting algorithm can provide more accurate results than Random Forests. They can detect intricate patterns in the data since we train them to rectify each other's error values. Random forests may not be as accurate as gradient enhancing trees. They can detect intricate patterns in the data because we train them to correct each other's mistakes. The boosted trees may overfit and begin modeling the noise if the data are noisy, though. The way they produce decisions is the other key distinction. A random forest's trees can choose their outputs in any order because each tree is independent. Then, we combine all of the individual forecasts into a single prediction, which is either the average value in regression issues or the majority class in classification questions. On the other hand, the order in which the gradient boosting trees run is set and cannot be altered. They only accept sequential assessment as a result.

From Table 3 it is observed that Random Forest classification-based algorithm results in the highest F1-Score of 1.00. Similarly, it is observed from the AUC curve as shown in Figure 2d, Random Forest has highest AUC score of 1.00. Figure 2c shows the confusion matrix of each classification-based algorithms. With the addition of separating on a random subset of characteristics, random forest outperforms bagging by decorrelating the trees. As a result, the model only takes into account a small subset of its properties at each branch in the tree rather than all of them. That is, a subset of the m features are randomly chosen from the set of n features that are available. This is crucial in order to average out volatility.

6. Conclusions

This paper presents a machine learning models for predicting the material removal rate of alloys NiTi, NiCu, and BeCu during EDM. The obtained experimental results were trained and tested on the supervised machine learning algorithms which were based on classification and regression models for predicting the material removal rate with higher accuracy. It is observed from the results that the Gradient boosting regression-based algorithm resulted in the highest coefficient of determination value while Random Forest classification based resulted in the highest F1-Score. Based on the analysis of results, it's found that pulse off time and workpiece electrical conductivity are least significant parameters. The most significant parameters that effect material removal rate are pulse on time, gap current and gap voltage. The future scope of this work is to integrate these machine learning models with the metaheuristics algorithms for the improvement in accuracy scores.

Author Contributions: Conceptualization, V.S.J. (Vijaykumar S. Jatti); methodology, V.S.J. (Vijaykumar S. Jatti); software, R.B.D.; validation, R.B.D.; formal analysis, A.M.; investigation, A.M.; resources, N.K.K.; data curation, V.S.J. (Vinaykumar S. Jatti); writing—original draft preparation, A.V.J.; writing—review and editing, V.S.J. (Vinaykumar S. Jatti); visualization, A.V.J.; supervision, V.S.J. (Vijaykumar S. Jatti); project administration, N.K.K.; funding acquisition, N.K.K. All authors have read and agreed to the published version of the manuscript.

Funding: This research received no external funding.

Data Availability Statement: Not applicable.

Acknowledgments: Thanks to college administration for supporting this work.

Conflicts of Interest: The authors declare no conflict of interest.

References

1. Ming, W.; Zhang, S.; Zhang, G.; Du, J.; Ma, J.; He, W.; Cao, C.; Liu, K. Progress in modeling of electrical discharge machining process. *Int. J. Heat Mass Transf.* **2022**, *187*, 122563. [CrossRef]
2. Shastri, R.K.; Mohanty, C.P.; Dash, S.; Gopal, K.M.P.; Annamalai, A.R.; Jen, C.P. Reviewing Performance Measures of the Die-Sinking Electrical Discharge Machining Process: Challenges and Future Scopes. *Nanomaterials* **2022**, *12*, 384. [CrossRef]
3. Boopathi, S. An extensive review on sustainable developments of dry and near-dry electrical discharge machining processes. *J. Manuf. Sci. Eng.* **2022**, *144*, 050801. [CrossRef]
4. Baroi, B.K.; Patowari, P.K. A review on sustainability, health, and safety issues of electrical discharge machining. *J. Braz. Soc. Mech. Sci. Eng.* **2022**, *44*, 59. [CrossRef]
5. Kannan, E.; Trabelsi, Y.; Boopathi, S.; Alagesan, S. Influences of Cryogenically Treated Work Material on Near-Dry Wire-Cut Electrical Discharge Machining Process. *Surf. Topogr. Metrol. Prop.* **2022**, *10*, 015027. Available online: https://iopscience.iop.org/article/10.1088/2051-672X/ac53e1 (accessed on 12 July 2022). [CrossRef]
6. Chaudhari, R.; Prajapati, P.; Khanna, S.; Vora, J.; Patel, V.K.; Pimenov, D.Y.; Giasin, K. Multi-response optimization of Al_2O_3 nanopowder-mixed wire electrical discharge machining process parameters of nitinol shape memory alloy. *Materials* **2022**, *15*, 2018. [CrossRef]
7. Karthik Pandiyan, G.; Prabaharan, T.; Jafrey Daniel James, D.; Sivalingam, V. Machinability analysis and optimization of electrical discharge machining in AA6061-T6/15wt.% SiC composite by the multi-criteria decision-making approach. *J. Mater. Eng. Perfor.* **2022**, *31*, 3741–3752. [CrossRef]
8. Vora, J.; Khanna, S.; Chaudhari, R.; Patel, V.K.; Paneliya, S.; Pimenov, D.Y.; Giasin, K.; Prakash, C. Machining parameter optimization and experimental investigations of nano-graphene mixed electrical discharge machining of nitinol shape memory alloy. *J. Mater. Res. Technol.* **2022**, *19*, 653–668. [CrossRef]
9. Akıncıoğlu, S. Taguchi optimization of multiple performance characteristics in the electrical discharge machining of the $TiGr_2$. *Facta Univ. Mech. Eng.* **2022**, *20*, 237–253. [CrossRef]
10. Danish, M.; Al-Amin, M.; Abdul-Rani, A.M.; Rubaiee, S.; Ahmed, A.; Zohura, F.T.; Ahmed, R.; Yildirim, M.B. Optimization of hydroxyapatite powder mixed electric discharge machining process to improve modified surface features of 316L stainless steel. *Proc. Inst. Mech. Eng. Part E J. Process Mech. Eng.* **2022**. [CrossRef]
11. Kam, M.; İpekçi, A.; Argun, K. Experimental investigation and optimization of machining parameters of deep cryogenically treated and tempered steels in electrical discharge machining process. *Proc. Inst. Mech. Eng. Part E J. Process Mech. Eng.* **2022**, *236*, 1927–1935. [CrossRef]
12. Gautam, N.; Goyal, A.; Sharma, S.S.; Oza, A.D.; Kumar, R. Study of various optimization techniques for electric discharge machining and electrochemical machining processes. *Mater. Today Proc.* **2022**, *57*, 615–621. [CrossRef]
13. Shukla, S.K.; Priyadarshini, A. Application of machine learning techniques for multi objective optimization of response variables in wire cut electro discharge machining operation. *Mater. Sci. For.* **2019**, *969*, 800–806. [CrossRef]
14. Ghosh, I.; Sanyal, M.K.; Jana, R.K.; Dan, P.K. Machine learning for predictive modeling in management of operations of EDM equipment product. In Proceedings of the Second International Conference on Research in Computational Intelligence and Communication Networks (ICRCICN), Kolkata, India, 23–25 September 2016; pp. 169–174. [CrossRef]
15. Ulas, M.; Aydur, O.; Gurgenc, T.; Ozel, C. Surface roughness prediction of machined aluminum alloy with wire electrical discharge machining by different machine learning algorithms. *J. Mater. Res. Tech.* **2020**, *9*, 12512–12524. [CrossRef]
16. Ali, M.A.; Samsul, M.; Hussein, N.I.S.; Rizal, M.; Izamshah, R.; Hadzley, M.; Kasim, M.S.; Sulaiman, M.A.; Sivarao, S. The Effect of Edm Die-sinking Parameters on Material Removal Rate of Beryllium Copper Using Full Factorial Method. *Middle-East J. Sci. Res.* **2013**, *16*, 44–50. [CrossRef]
17. Selvakumar, G.; Sarkar, S.; Modern, S.M.I.J. Experimental analysis on WEDM of monel 400 alloys in a range of thicknesses. *Int. J. Mod. Manuf. Technol.* **2012**, *4*, 113–120.
18. Kumar, V.; Kumar, V.; Kumar, K. An experimental analysis and optimization of machining rate and surface characteristics in WEDM of Monel-400 using RSM and desirability approach. *J. Ind. Eng. Int.* **2015**, *11*, 297–307. [CrossRef]
19. Kumar, N.E.A.; Babu, A.S. Influence of input parameters on the near-dry WEDM of Monel alloy. *Mater. Manuf. Process.* **2018**, *33*, 85–92. [CrossRef]
20. Daneshmand, S.; Kahrizi, E.F.; Abedi, E.; Abdolhosseini, M.M. Influence of machining parameters on electro discharge machining of NiTi shape memory alloys. *Int. J. Electrochem. Sci.* **2013**, *8*, 3095–3104.
21. Gangele, A.; Mishra, A. Surface roughness optimization during machining of NiTi shape memory alloy by EDM through Taguchi's technique. *Mater. Today Proc.* **2020**, *29*, 343–347. [CrossRef]
22. Daneshmand, S.; Monfared, V.; Neyestanak, A.A.L. Effect of tool rotational and Al_2O_3 powder in electro discharge machining characteristics of NiTi-60 shape memory alloy. *Silicon* **2016**, *9*, 273–283. [CrossRef]
23. Pogrebnjak, A.D.; Bratushka, S.N.; Beresnev, V.M.; Levintant-Zayonts, N. Shape memory effect and superelasticity of titanium nickelide alloys implanted with high ion doses. *Russ. Chem. Rev.* **2013**, *82*, 1135–1159. [CrossRef]